Electrochemical Studies in HNO_3–N_2O_4 Mixtures: Corrosion of Stainless Steel in HNO_3–N_2O_4 Mixtures and the Effect of Inhibitors

Paul G. Cheeseman, Michael F. A. Dove,* Richard C. Hibbert, and Norman Logan
Department of Chemistry, University of Nottingham, University Park, Nottingham NG7 2RD
Peter J. Boden
Department of Metallurgy, University of Nottingham, University Park, Nottingham NG7 2RD

Electrochemical studies demonstrate that a rhodium wire can be used as a reference electrode in HNO_3–N_2O_4 mixtures. The electrode reaction $NO_2^+ + e^- \rightleftharpoons \frac{1}{2}N_2O_4$ occurs on the rhodium surface. Platinum can also be used as a reference electrode, although its performance is slightly inferior to rhodium. Electrochemical studies using this reference system indicate that stainless steels corrode in HNO_3–N_2O_4 mixtures by a mechanism involving transpassive breakdown. This breakdown is prevented by cathodic polarisation or by addition of fluoride or phosphorus pentafluoride. The results are consistent with fluoride functioning as an anodic film-forming inhibitor. Sulphuric acid also functions as an inhibitor but its performance is less satisfactory than that of fluoride.

Fuming nitric acids have found widespread use as the oxidiser component of liquid bipropellant systems. In common current use are 'high density acid'[1] (HNO_3–N_2O_4, 56:44 w/w) and 'red fuming nitric acid' (HNO_3–N_2O_4–H_2O, 84.5:14:1.5 w/w). Because of their highly corrosive nature, high density acid (hda) and red fuming nitric acid (rfna) usually contain HF (*ca.* 0.7 wt.%) as inhibitor.

The present work arose out of our interest in studying redox reactions and corrosion processes in fuming nitric acids by electrochemical methods. In particular, we were interested in developing a suitable reference system for use in these media.

In 100% HNO_3 there is no evidence for the existence of the hydroxonium ion (H_3O^+). The nitronium ion (NO_2^+) is believed to be the species responsible for the corrosive and highly oxidising behaviour, NO_2^+ being produced from the self-ionisation of nitric acid,[1] equation (1).

$$2HNO_3 \rightleftharpoons NO_2^+ + NO_3^- + H_2O \quad (1)$$

When dissolved in nitric acid, dinitrogen tetroxide (N_2O_4) is almost completely ionised, equation (2), up to a concentration

$$N_2O_4 \rightleftharpoons NO^+ + NO_3^- \quad (2)$$

of 1.6 mol kg^{-1}.[2] N_2O_4 and NO_2 are present as molecular species in these solutions but their concentrations are very low.[2] The presence of both NO_2^+ and N_2O_4 in HNO_3–N_2O_4 mixtures is significant since they are related by the redox equilibrium (3).

$$NO_2^+ + e^- \rightleftharpoons \tfrac{1}{2}N_2O_4 \quad (3)$$

The electrochemistry of the HNO_3–N_2O_4 system has been briefly examined by Lee and Millen[3] who identified, in addition to the cathodic reaction (4), two anodic reactions (5) and (6).

$$NO_2^+ + e^- \longrightarrow \tfrac{1}{2}N_2O_4 \quad (4)$$

$$\tfrac{1}{2}N_2O_4 \longrightarrow NO_2^+ + e^- \quad (5)$$

$$NO_3^- \longrightarrow NO_2^+ + \tfrac{1}{2}O_2 + e^- \quad (6)$$

Reaction (5) occurred preferentially when there was sufficient N_2O_4 in solution. Harrar and Pearson[4] studied the electrolysis of HNO_3–N_2O_4 mixtures on platinum metal and iridium oxide using a calomel reference electrode. Upon oxidation they noted conversion of N_2O_4 to N_2O_5 consistent with equation (5). However, their polarisation curves did not display clearly defined Tafel regions.

The work reported here shows that more quantitative information can be obtained by electrochemical polarisation of the redox equilibrium (3). Because of the relatively high exchange current density and the Tafel slopes close to theory, there is every confidence in rhodium as a reference electrode in fuming nitric acids. Studies involving platinum demonstrate that it can also be used as a reference electrode, although its performance is inferior to rhodium. We also report the results of electrochemical studies upon corrosion and inhibition of 321 and 347 stainless steels in HNO_3–N_2O_4 mixtures.

Experimental

The preparation and handling of PF_5, HNO_3, N_2O_4, and hda have been described previously;[5] rfna was propellant grade quality supplied by the Ministry of Defence, Propellants, Explosions, and Rocket Motors Establishment, Westcott.

Potential–current curves were recorded directly using either a Wenking model PCA 72 or a Thompson Ministat precision potentiostat and a Bryans *X–Y* recorder. The Wenking was driven by a Chemical Electronics Co. linear sweep generator and the Ministat by a DRG 16 digital linear sweep generator. Scan rates were in the range 10^{-1} to 10^{-4} mV s^{-1}. Polarisation curves were also recorded using a staircase waveform. The potential function was produced by a specially designed generator. The current was automatically recorded at each potential using a Keithly 750 printer. Using the potential step generator, the interval between potential steps could be varied from 1 to 1 000 s and the magnitude of the potential increment could be varied from 1 to 100 mV. Potential measurements were carried out using a high impedance DM 450 Sinclair multimeter.

Conventional electrochemical cell designs and procedures were employed in initial studies.[6] It was subsequently found that cell design had little influence upon the shape of potential–current curves. Studies involving fluoride-inhibited media were carried out in a specially designed cell (Figure 1).

Rhodium (1 mm diameter) and platinum (0.5 mm diameter) wires (Johnson-Matthey) were used as reference and working electrodes. The auxiliary electrode was a platinum flag (0.5 cm × 0.5 cm). Stainless steel working electrodes were abraded with a series of silicon carbide abrasive papers before polishing on 8 and 1 μm diamond wheels.

Potential measurements for the HNO_3–N_2O_4 system were

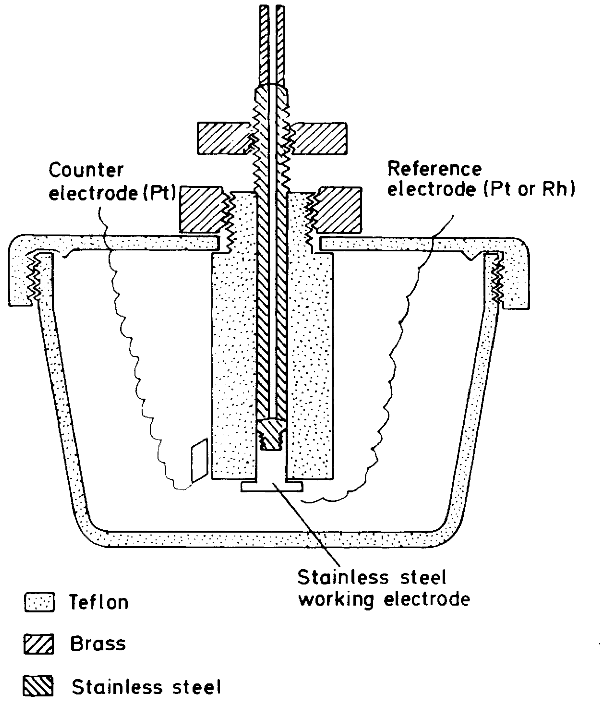

Figure 1. Fluoroplastic electrochemical cell

carried out in a three-compartment, two-electrode cell. The reference electrode compartment was separated from the main cell by a conducting bridge of 100% HNO_3 and two sintered glass discs. The electrodes were rhodium wires (1 mm diameter, 2 mm length) sealed into fluoroplastic tubing and spot-welded to platinum for the external connection. N_2O_4 solution (0.1 mol kg^{-1}) was placed in the reference cell compartment. This composition was chosen as an arbitrary zero. HNO_3 was placed in the main cell compartment to which N_2O_4 in HNO_3 (0.043 mol kg^{-1}) was added in portions from a burette. The cell was maintained at 0 °C to help eliminate temperature effects caused by the heat of solution of N_2O_4.[7] The potential at N_2O_4 concentrations between 10^{-4} and *ca.* 1 mol kg^{-1} in the main cell was recorded relative to the 0.1 mol kg^{-1} solution. A time interval of 1 min between additions was found to be sufficient to allow the system to equilibrate.

Results and Discussion

(*a*) *Studies using Platinum and Rhodium Working Electrodes.*—Linear potential–log current (Tafel) plots were obtained for all HNO_3–N_2O_4 mixtures, up to 50% N_2O_4, using rhodium as both the working and reference electrodes. Anodic Tafel slopes at 0 °C were in the range +110 to +150 mV and cathodic slopes were between −110 and −120 mV. The experimental values compare well with the theoretical values of +108 and −108 mV for a single electrode process assuming a transfer coefficient (β) value of 0.5.

Extrapolation of either the anodic or the cathodic Tafel slopes yielded exchange current density values (i_0) in the range 150—170 µA cm^{-2}. The agreement between i_0 (anodic) and i_0 (cathodic) was excellent. Non-Tafel behaviour was observed upon anodic polarisation of 100% HNO_3 or of HNO_3–N_2O_4 mixtures where the N_2O_4 concentration was less than *ca.* 10^{-4} mol kg^{-1}. The Tafel plot for rhodium in rfna gave similar Tafel slopes (at 22 °C) of +108 mV (anodic) and −95 mV (cathodic) (theoretical: ±117 mV for $\beta = 0.5$). The potential–current curves for all media showed little hysteresis and displayed essentially no dependence upon scan rate.

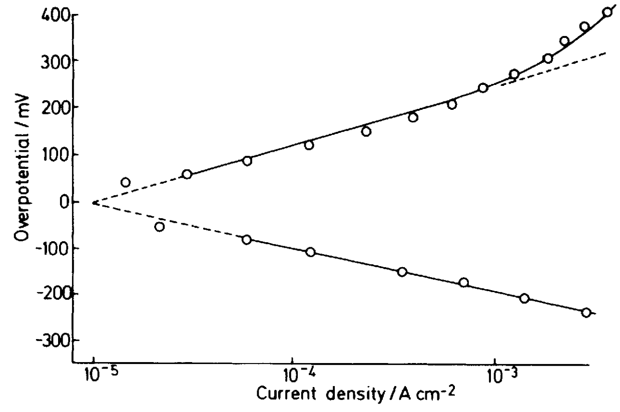

Figure 2. Tafel plot for a platinum electrode in hda

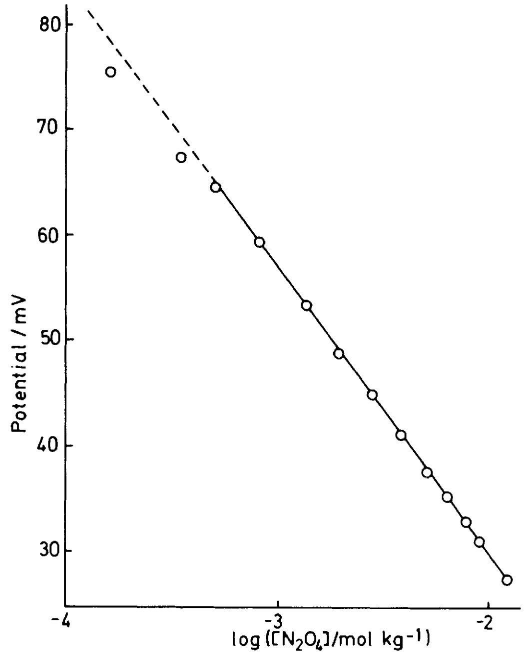

Figure 3. Potential (*vs.* 0.1 mol kg^{-1} N_2O_4 in HNO_3) as a function of added N_2O_4 concentration

The polarisation behaviour of platinum (Figure 2) was similar to that of rhodium, although the exchange current density values were generally an order of magnitude lower on platinum compared to rhodium.

In all media, both anodic and cathodic concentration polarisation was observed at overvoltages in excess of *ca.* ±300 mV.

The Nernst equation for the $NO_2^+/\frac{1}{2}N_2O_4$ couple for low concentrations of N_2O_4 can be written as in equation (7). At low

$$E = E^\circ + \frac{2.303\,RT}{F}\log\left[\frac{a_{NO_2^+}}{(a_{N_2O_4})^{\frac{1}{2}}}\right] \qquad (7)$$

concentrations of N_2O_4 the activity of the nitronium ion ($a_{NO_2^+}$) will be effectively independent of N_2O_4 concentration as a consequence of the extensive self-ionisation of HNO_3 [equation (1)] and the activity of N_2O_4 ($a_{N_2O_4}$) may be taken as directly proportional to the added N_2O_4 concentration ($[N_2O_4]_{add}$). This leads to equation (8) where K_1 is a constant.

$$E = E^{\circ} + \frac{2.303\ RT}{2F}\log\left(\frac{K_1}{[N_2O_4]_{add}}\right) \quad (8)$$

Equation (8) predicts that a plot of electrode potential against log $[N_2O_4]$ will be linear with slope $-2.303\ RT/2F$ (= −27 mV at 0 °C). For $[N_2O_4]_{add}$ values between 0.001 and 0.01 mol kg^{-1} (Figure 3) a linear plot with slope −27 ± 0.5 mV was in fact obtained, demonstrating that the $NO_2^+/\frac{1}{2}N_2O_4$ couple obeys the Nernst equation.

At $[N_2O_4]_{add} > 1$ mol kg^{-1} the NO_3^- generated by the ionisation of N_2O_4 [equation (2)] reduces the concentration of NO_2^+ significantly by suppressing the self-dissociation of HNO_3 [equation (1)] and a more complex treatment is required.

The polarisation studies and potential measurements demonstrate that the couple $NO_2^+/\frac{1}{2}N_2O_4$ on a rhodium wire surface fulfils the criteria[8] required of a reference electrode system. This was further demonstrated by comparing the potential–current curves obtained with a platinum electrode in rfna using rhodium and calomel reference electrodes. The two curves were essentially identical. Although rhodium has superior characteristics to platinum, it has been found in practice that studies in HNO_3–N_2O_4 mixtures are unaffected by substituting platinum for rhodium as a reference electrode.

(*b*) *Studies using* 321 *and* 347 *Stainless Steel Working Electrodes.*—Previous corrosion studies[9] in uninhibited HNO_3–N_2O_4 media have established that after an induction period, stainless steels corrode at a rate determined by the N_2O_4 and H_2O content of the medium. Corrosion takes place principally at the grain boundaries.

Corrosion can be inhibited by the addition of *ca.* 0.7 wt.% HF. A number of other substances also act as inhibitors. PF_5 appears to be the most useful alternative to HF. Polarisation and potential–time studies were undertaken in order to investigate the mechanisms of corrosion and inhibition in HNO_3–N_2O_4 mixtures.

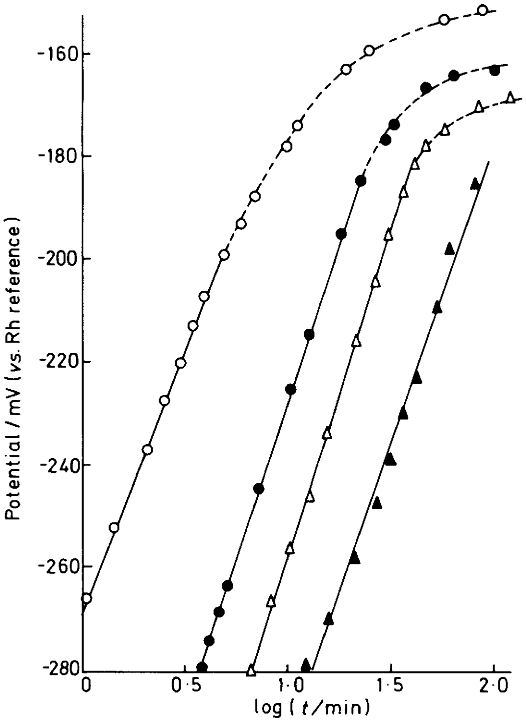

Figure 4. Potential–time (*t*) plots for 321 stainless steel in 14 wt.% N_2O_4 in HNO_3 as a function of added H_2SO_4: (○) 0, (●) 0.9, (△) 1.4, (▲) 3.0 wt.% H_2SO_4

Studies were carried out either in a conventional three-compartment, three-electrode (stainless steel working electrode, rhodium reference and platinum counter electrode) cell or in a specially designed fluoroplastic cell (see Figure 1). Current–potential curves for uninhibited media were very similar for both cell designs.

When immersed in uninhibited HNO_3–N_2O_4 mixtures, the potential of stainless steel working electrodes became more positive, indicating film formation until a certain critical potential is reached. The curve for 321 stainless steel in 14 wt.% N_2O_4 may be regarded as typical (Figure 4). A plot of potential (*E*) against log *t* is linear until the critical point is reached.

The linear portion of the plot corresponds to the induction period and indicates that initially the surface film is thickening and inhibiting the anodic reaction. At the critical potential film breakdown occurs. Breakdown can be initiated by polarising the stainless steel anodically (Figure 5). Increasing the anodic overpotential strips off the passive film (shown to be predominantly Cr_2O_3 at its outer surface by scanning electron microscopy).[10] On depolarisation the film is thinner at any given potential compared to its thickness at that same potential during polarisation and so the curve displays considerable hysteresis.

The potential–time and anodic polarisation studies can be explained by postulating that transpassive breakdown is occurring for stainless steels in HNO_3–N_2O_4 mixtures. After an induction period, in which the Cr_2O_3 film thickens, oxidation to non-protective chromium(VI) oxide takes place. The chromium(VI) oxide, unlike Cr_2O_3, is soluble in HNO_3–N_2O_4 mixtures and film breakdown occurs.

Cathodic protection. This breakdown can be retarded by polarising the stainless steel cathodically. Cathodic protection of a 321 stainless steel electrode in N_2O_4 solution (0.9 mol kg^{-1}) was carried out by applying a constant potential, using a potentiostat. An identical specimen was allowed to corrode without protection as a control.

After 11 d at 0 °C, the control specimen had acquired the characteristic black appearance associated with serious corrosion, also showing extensive intergranular attack with whole grains falling out from the surface. The specimen had lost weight and the solution had changed colour. In contrast, the cathodically protected specimen was found to be visually unchanged and lost no weight. The colour of the protected specimen solution was also unchanged.

Effect of H_2SO_4. Potential–time curves for 321 stainless steel in 14 wt.% N_2O_4–HNO_3 for different amounts of H_2SO_4 inhibitor are illustrated in Figure 4. With increasing additions of H_2SO_4 the curves indicate that build-up of the surface film is increasingly retarded. The general shape of polarisation curves

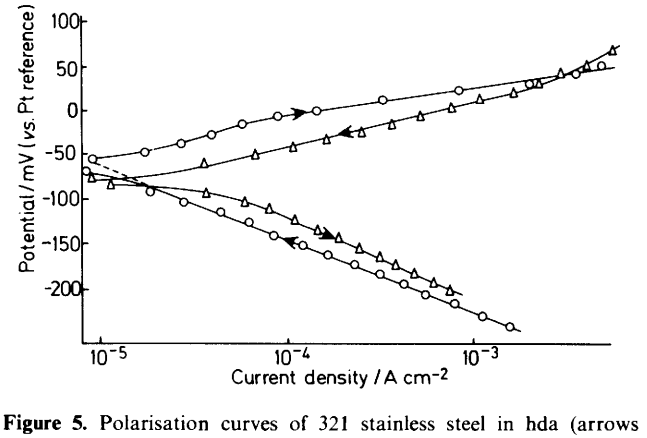

Figure 5. Polarisation curves of 321 stainless steel in hda (arrows indicate direction of polarisation)

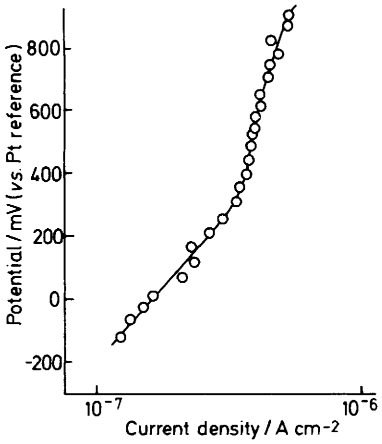

Figure 6. Potentiodynamic plot for 321 stainless steel in HF-inhibited hda

for sulphate-inhibited media were similar to those observed for stainless steel in uninhibited media. Optical microscopy of electrodes exposed to this polarisation breakdown showed an electrode surface covered with pits. The presence of the sulphate anion prevents intergranular attack but is shown to be an aggressive anion in the system, causing pitting corrosion of stainless steel.

Fluoride inhibition. Potential–time curves for fluoride-inhibited (added as either KF or HF) media were similar to those observed for H_2SO_4-containing systems but film formation seemed to be slower. The potentiodynamic curves (Figure 6) demonstrate that stainless steel is passivated in fluoride containing HNO_3–N_2O_4 mixtures even at high anodic overpotentials. We attribute this phenomenon to the formation of metal fluorides at the anodic sites on the metal surface. *X*-Ray photoelectron spectroscopy has demonstrated [10] the presence of substantial amounts of fluoride in the surface film on stainless steel after both brief and extended periods of immersion in HF-inhibited media.

Potentiodynamic curves for hda containing PF_5 were virtually identical to those obtained for HF-containing solutions. PF_5 is known [5] to generate HF, HPO_2F_2, PF_6^-, and some H_2PO_3F in hda. Inhibition due to the formation of anodic films is undoubtedly taking place in PF_5-containing solutions which probably involves the agency of both HF and fluorophosphoric acids.

More detailed electrochemical studies, including the use of cyclic voltammetry, into the nature of electrochemical processes in pure HNO_3 and HNO_3–N_2O_4 mixtures are currently in progress.

Conclusions

These can be summarised as follows.

(*i*) Electrochemical tests show that rhodium or platinum metal in HNO_3–N_2O_4 mixtures is a suitable reference electrode.

(*ii*) The presence of NO_2^+ in HNO_3–N_2O_4 mixtures, analogous to H^+ in aqueous acid solutions, provides a cathodic reaction which polarises stainless steel to a positive potential where the protective film, mainly Cr_2O_3, is oxidised to give a soluble Cr^{VI}-containing film.

(*iii*) Stainless steel can be cathodically protected in HNO_3–N_2O_4 mixtures.

(*iv*) Electrochemical tests showed that both HF and PF_5 formed protective films which were unaffected by the anodic polarisation induced by the redox reaction (3).

(*v*) Addition of sulphuric acid stopped intergranular attack but did not produce a sufficiently effective film, and pitting corrosion occurred.

Acknowledgements

We thank the S.E.R.C. for maintenance grants (to P.G.C. and R.C.H.), Johnson-Matthey Ltd., for the loan of ruthenium metal, and the Ministry of Defence, for a supply of red fuming nitric acid.

References

1 C. C. Addison, *Chem. Rev.*, 1980, **80**, 21.
2 J. D. S. Goulden and D. J. Millen, *J. Chem. Soc.*, 1950, 2620.
3 W. H. Lee and D. J. Millen, *J. Chem. Soc.*, 1958, 2248.
4 J. E. Harrar and R. K. Pearson, *J. Electrochem. Soc.*, 1983, **130**, 108.
5 C. C. Addison, J. W. Bailey, S. H. Bruce, M. F. A. Dove, R. C. Hibbert, and N. Logan, *Polyhedron*, 1983, **2**, 651.
6 J. A. Von Fraunhofer and C. H. Banks, 'Potentiostat and its Applications,' Butterworths, London, 1972.
7 W. H. Lee, 'The Chemistry of Non-Aqueous Solvents,' ed. J. J. Lagowski, Academic Press, London, 1967, vol. 2.
8 D. J. G. Ives and G. T. Janz, 'Reference Electrodes,' Academic Press, London, 1969.
9 D. M. Tallet and N. Logan, unpublished work.
10 P. G. Cheeseman and M. F. A. Dove, unpublished work.

Received 4*th September* 1984; *Paper* 4/1530